

Study on Seismic Dynamic Response and Failure Mode of Metro Station Affected by Burial Depths

S. Huang., Y. Peng and Y. Lyu

Institute of Crustal Dynamics, China Earthquake Administration, Beijing

Email: huangshuai3395@163.com

ABSTRACT: The metro station structure shows different failure modes when it is located at different burial depths. This research work is aimed to determine the influence laws of burial depths on dynamic response and failure modes of the metro station under near and far field earthquakes based on the nonlinear elastic-plastic finite element model of the metro station. The research results show that the horizontal displacements and acceleration dynamic magnification factors of the metro station decrease and especially the internal forces increase gradually when the burial depth increases. The decreasing amplitude of the horizontal displacements and acceleration dynamic magnification factors of the metro station is reduced and the increasing amplitude of the internal forces slows down when the burial depth increases to a specific extent. Therefore, desirable anti-seismic performance could be achieved when a specific range of burial depth is avoided reasonably. At last, indoor shaking table test for metro station was done, through which we determined the initial failure position and the failure mode of the metro station under earthquake. And shaking table test results demonstrate the validation of the numerical simulation results.

KEYWORDS: Burial depth, Metro station, Near and far field earthquakes, Shaking table test, Failure mode.

1 INTRODUCTION

Metro stations are located on urban trunk roads or in urban residential areas, business districts or the most populous areas in general. In case of a devastating disaster, it may generate a chain and scale effect, leading to aggravated hazards and a series of very serious infrastructure damages, such as cracking of neighboring buildings and rupture of underground pipelines. In recent years, seismic actions have triggered damage of a great many underground structures[1][2]. For example, the Great Kanto Earthquake in Japan in 1923 (M8.2) destroyed 82 tunnels in the earthquake region; the Kern Earthquake in California, the United States in 1952 (M7.6) seriously damaged four tunnels of the Southern Pacific Railroad; the Izu Earthquake in Japan in 1978 (M7.0) resulted in fractures across tunnels and a series of damage of the tunnel lining; particularly, the Great Hanshin Earthquake in Japan in 1995 (M7.2) ruined some underground metro stations and section tunnels in Kobe. In Dakai Station, more than a half of the central columns were completely toppled down, resulting in roof collapse and enormous sedimentation of the overlying soil. The massive earthquake damage of metro underground structure has gradually aroused people's attention to its seismic safety.

Following the increase of underground structure and the frequent appearance of seismic damage of underground structure, the issue of earthquake resistance of underground structures is attracting more attention of seismologists in all countries of the world. For ground structure, the changes in the shape, mass and stiffness of the structure have great influence on structure response. For underground structure, the kinetic characteristics of the foundation is a major factor influencing structure response, so it is unreasonable to consider static method as a basis of the seismic design of underground structure[3]. China is relatively backward in seismic research of underground structure and still does not have a sound seismic analysis method for underground structure by now, so further research and development is needed in the seismic design theories and methods regarding to underground structure.

The dynamic characteristics of metro station are controlled by the surrounding foundation soil. Meanwhile, foundation soil is also influenced by underground structure, so it is necessary to take account of the interaction between soil and structure[4]. Hashasha[5] pointed out that when underground structure shakes at a low level under low-intensity seismic action or is in hard rock or other media, the results calculated by quasi-static method are acceptable. Otherwise, the influence of structure-soil interaction on underground structure should not be neglected. G.Gazetas[6] studied the influence of

structure-soil interaction on the dynamic response of underground structure under seismic action, and concluded that the influence of structure-soil interaction on underground structure cannot be neglected. Youssef M.A. Hashasha [7] stated that when underground structure shakes at a low level under low-intensity seismic action or is in hard rock or other media, the results calculated by quasi-static method are acceptable. Otherwise, the influence of structure-soil interaction on underground structure should not be neglected. Furthermore, the seismic resistance of the metro station also affected by structural burial depth, making the anti-seismic research of the underground structure more complex [8] [9].

In this study, considering soil-structure interaction, the influence laws of burial depths on seismic dynamic response of metro station are studied based on a nonlinear elastic-plastic finite element model of metro station. And we also analyze the failure mode of metro station through an indoor shaking table test, which is expected to provide reference and guidance value for engineering practice.

2 CALCULATION MODEL

2.1 Establishment of a numerical simulation model

A rectangular metro structure is selected as a research object. The metro station structure is 22m wide, 15m high and 1m thick, the calculation area of the structural part is 22m×15m, and the burial depth of the station is 20m. The artificial boundary of the calculation site is twice of the width of the metro structure. The distance of the artificial boundary from a bottom side to a bottom side of the metro station is 25m, in other words, the width is 110m and the depth (including structure) is 60m. The metro structure was treated as single-phase medium. The

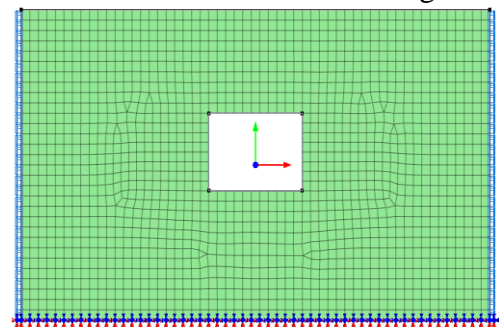
Table 1 – Physical and mechanics parameters

| Name | Density(kg/m ³) | Modulus of Elasticity (GPa) | Shear modulus (GPa) | Poisson's ratio | Cohesion (kPa) | Internal friction angle(°) | Yield strength (N/mm ²) |
|---------------|-----------------------------|-----------------------------|---------------------|-----------------|----------------|----------------------------|-------------------------------------|
| Site soil | 2100 | 0.54 | 0.36 | 0.25 | 44 | 27 | \ |
| Interlayer | 2650 | 0.01 | 0.004 | 0.3 | 10 | 15 | \ |
| Metro station | 2500 | 17.3 | 11.5 | 0.20 | \ | \ | 10 |

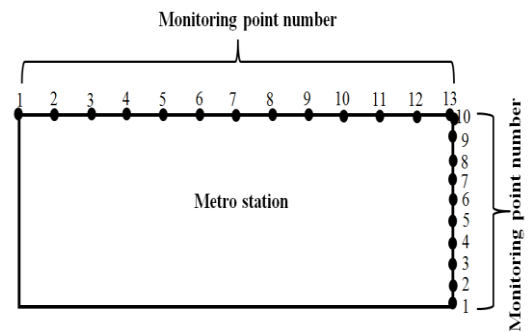
2.2 Selection of seismic waves

The basic intensity of the region of the slope is 8 degrees, and the site is II. The basic acceleration value of severe earthquake is 0.21g, and the peak accelerations of the seismic waves are adjusted for 0.21g. Refer to *Japanese Specifications for Highway*

soil constitutive model adopted Mohr-Coulomb, the station structure adopted a linear elastic constitutive model, and meanwhile Rayleigh damping was selected to simulate damping effect [10]. Soil and metro station structure both adopted rectangular grid 1m×1m with plane strain model. The left boundary, right boundary and bottom boundary of the model all adopted free field boundaries. In the calculation process, no disengagement and slump between soil and structure were considered, and only complete cohesion between them was considered. The numerical simulation model and distribution of monitoring points for metro station are shown in Figure 1.



a) Numerical simulation model



b) Distribution of monitoring points

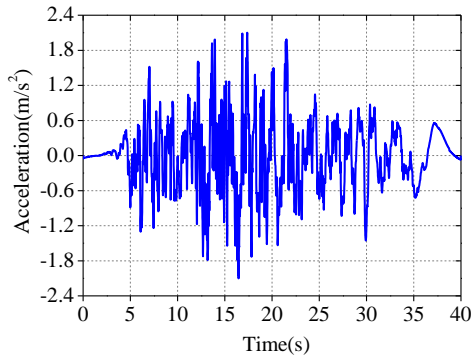
Figure 1 -Numerical simulation model and monitoring points

Physical parameters of site soil and station structure are as shown in Table 1.

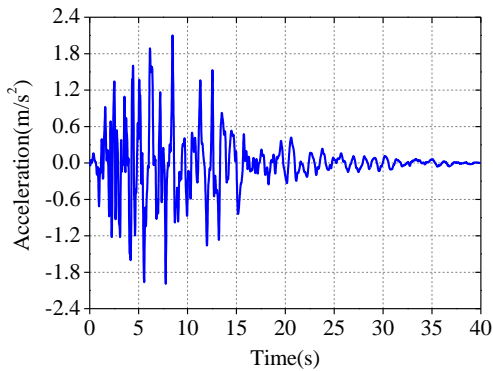
Bridges[11], the far field seismic waves (Type I: T1-II-1) and the near field seismic waves (Type II: T2-II-1) and EICentro seismic waves are chose, and the basic characteristics of seismic records are shown in Table 2. The acceleration time- histories of the seismic waves are shown in Figure.2.

Table 2 – Basic characteristics of seismic records

| Type No | Name of earthquake | Magnitude | Distance to epicenter/km | Place of record | Acceleration peak/Gal |
|---------|-------------------------------|-----------|--------------------------|--------------------------|-----------------------|
| T1-II-1 | Hyūga-nada Earthquake in 1968 | 7.5 | 100 | Bandao Bridge Foundation | 318.84 |
| T2-II-1 | Kobe Earthquake in 1995 | 7.2 | 11 | JR Yingqu Station | 686.83 |



a) T1-II-1



b) T1-II-1

Figure 2 –Time history of seismic wave

Fourier Transform is conducted for different seismic waves to obtain the response spectra of different seismic waves, as shown in Figure 3.

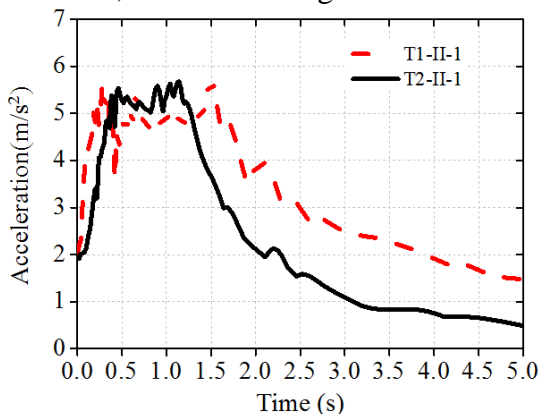


Figure 3 –Seismic response spectrum

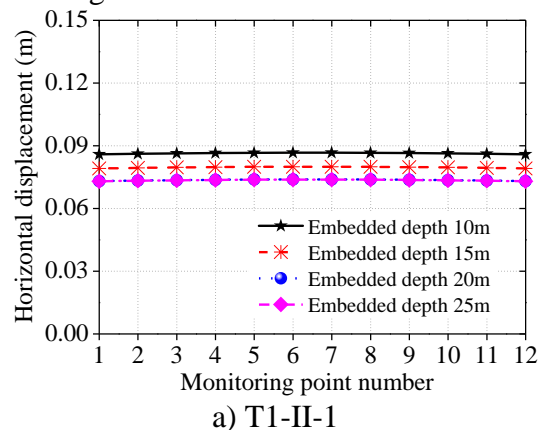
As shown in Figure 3, the response spectrum curves are drawn for five seismic waves when the damp is 5%. The spectral values corresponding to T1-II-1 (Type1) are distributed in period 0.25~1.5s in a centralized way. The distribution of the periodic domain is wide, and the acceleration response declines slowly with the increase of natural vibration period. For

T2-II-2 (Type2), the platform of the predominant period of acceleration response spectrum is short, and the corresponding spectral values are mainly distributed in period of 0~0.8s in a centralized way. With the increase of the structural natural period of vibration, the response acceleration reduces faster than T1-II-1 seismic waves.

3 INFLUENCE LAWS OF BURIAL DEPTH ON DYNAMIC RESPONSE OF THE METRO STATION

In the analysis of seismic response, we are more interested in maximum node displacement, dynamic amplification factor and structural internal forces (bending moment, shearing force and axial force), so we selected the roof and side wall (the left and right side walls are symmetric) of the metro station for comparative analysis.

In order to study the influence laws of the burial depth on the seismic dynamic response of the metro station, we chose roof position as a calculation point and the burial depths are 10m, 15m, 20m and 25m. The maximum horizontal displacements of the roof and side wall of the metro station are shown in Figure 4 and Figure 5.



a) T1-II-1

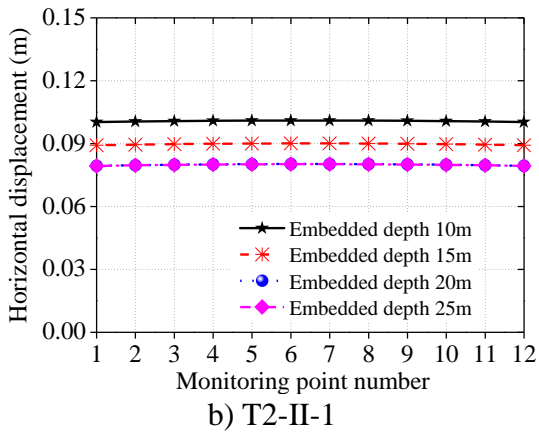
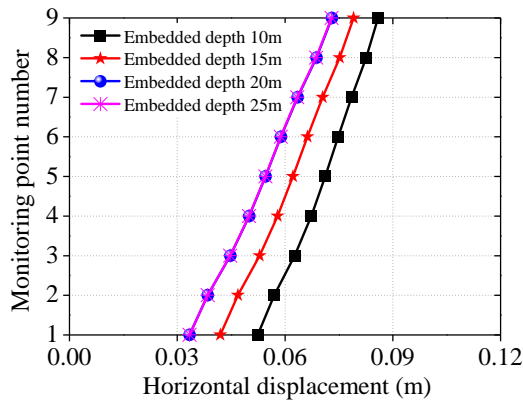
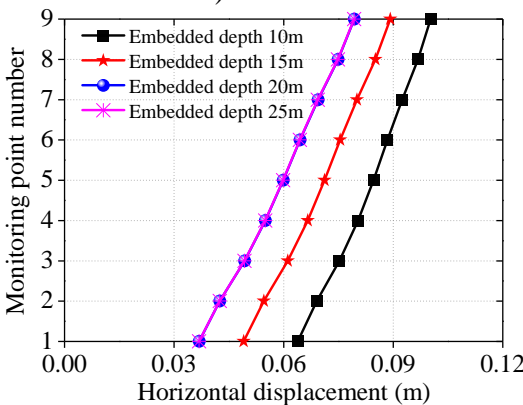


Figure 4 –The maximum horizontal displacement of the roof under near and far field earthquakes



a) T1-II-1



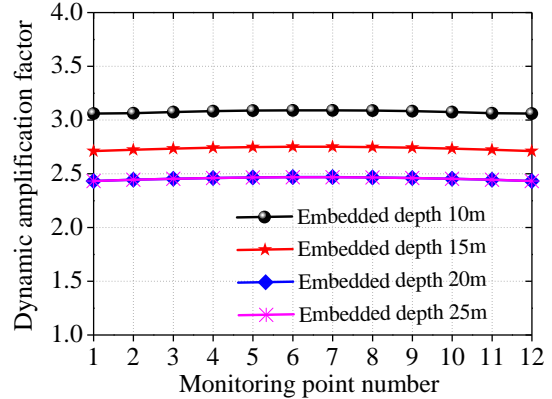
b) T2-II-1

Figure 5 –The maximum horizontal displacement of the side wall under near and far field earthquakes

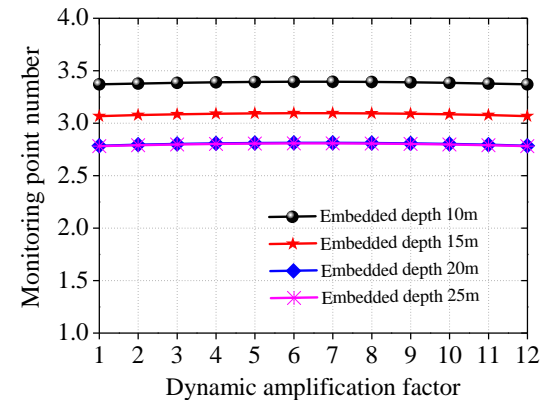
As shown in Figure 4 and Figure 5, with the increase of the burial depth of the metro station, the horizontal displacements of the roof and side wall show a decreasing trend under T1-II-1 and T2-II-1 earthquakes, indicating that the greater the burial depth of the metro station is, the less the deformation will be. The maximum horizontal displacement of the roof decreases about 22%, and the maximum horizontal displacement of the side wall decreases about 56% under T1-II-1 earthquake when the burial depth is from 10m to 25m. The maximum horizontal displacement of the roof decreases about 44%, and the maximum horizontal displacement of the side wall decreases about 63% under T2-II-1 earthquake when

the burial depth of the metro station structure is from 10m to 25m. When the burial depth reaches 20m, its influence on the deformation of the metro station structure will decrease with the increase of the burial depth. Therefore, the burial depth has a large influence on the deformation of metro station in a specific range, and the influence of burial depth on the deformation of the metro station could be omitted after a specific value of the burial depth.

The acceleration dynamic amplification factor could more intuitively reflect the dynamic amplification effect of the site on the metro station structure. And the maximum horizontal acceleration dynamic amplification factors of the metro station are shown in Figure 6 and Figure 7.

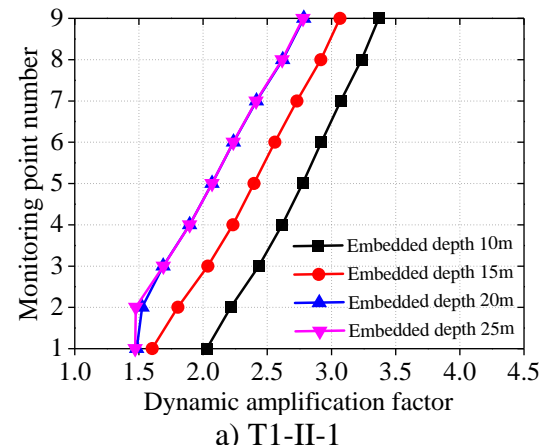


a) T1-II-1



b) T2-II-1

Figure 6 –The maximum horizontal acceleration dynamic magnification factors of the roof under near and far field earthquakes



a) T1-II-1

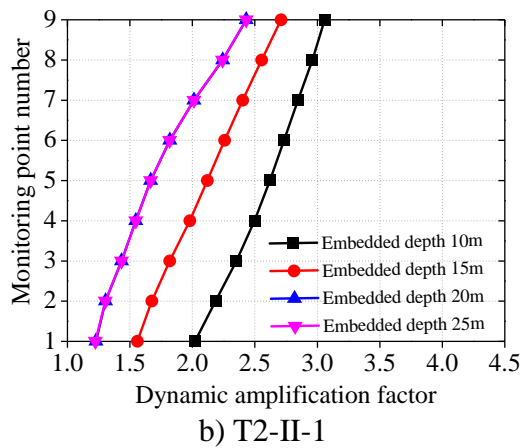


Figure 7 –The maximum horizontal acceleration dynamic magnification factors of the side wall under near and far field earthquakes

As shown in Figure 6 and Figure 7, with the increase of the burial depth of the metro station, the acceleration dynamic amplification factors of the roof and side wall decrease under T1-II-1 and T2-II-1 earthquakes. Thus, the increase of the burial depth may alleviate the vibration effect of the metro station under seismic action. The influence of the burial depth on the dynamic amplification factor of the metro sta-

tion decrease when the burial depth reaches 20m, which shows that after the burial depth reaching a specific value, its influence on dynamic amplification factor of the metro station could be omitted. The dynamic amplification factor of the roof decreases about 22% at most and the dynamic amplification factor of the side wall decreases about 28% at most under T1-II-1 earthquake when the burial depth of the metro station structure is from 10m to 25m. The dynamic amplification factor of the roof decreases about 29% at most, and the dynamic amplification factor of the side wall decreases about 60% at most under T2-II-1 earthquake when the burial depth of the metro station structure is from 10m to 25m. Therefore, near-field earthquake has greater influence on the dynamic amplification factor of the metro station than that under far-field earthquake.

In order to study the influence of burial depth on the internal forces (shearing force, bending moment and axial force) of the metro station, the internal forces of the metro station are calculated when the burial depths are 10m, 15m and 25m respectively, as shown in Table 3.

Table 3 –The maximum internal force of metro station structure in different embedment depth

| Embedment depth (m) | T1-II-1 | | | T2-II-1 | | |
|---------------------|------------------|-----------------------|------------------|------------------|-----------------------|------------------|
| | Shear force (kN) | Bending moment (kN·m) | Axial force (kN) | Shear force (kN) | Bending moment (kN·m) | Axial force (kN) |
| 10 | 1108 | 2122 | 2078 | 1173 | 2229 | 2234 |
| 15 | 1162 | 2240 | 2189 | 1260 | 2415 | 2391 |
| 20 | 1183 | 2281 | 2201 | 1282 | 2443 | 2413 |
| 25 | 1197 | 2308 | 2247 | 1291 | 2481 | 2433 |

As shown in Table 3, with the increase of the burial depth, the internal forces of the metro station increase gradually under near and far-field earthquake. The bending moments, shearing forces and axial forces at all critical nodes of the metro station increase with the increasing of the burial depth. The increase amplitude of the bending moments, shearing forces and axial forces at all critical nodes of the metro station decreases obviously when the burial depth is from 20m to 25m. The shearing force of the metro station increases 8%, bending moment increases 9%, and axial force increases 8% under T1-II-1 when the burial depth increases from 10m to 25m. The shearing force of the metro station increases 10%, bending moment increases 11%, and axial force increases 9% under T2-II-1 when the burial depth increases from 10m to 25m. Thus, near field earthquake has greater influence on the internal forces of the metro station than that under far field earthquake. With the increase of burial depth, the in-

fluence of earthquakes on the internal forces of the metro station decreases. Because of the increasing of the overlying site pressure, the internal forces of the metro station increase gradually. Therefore, the influence of the overlying site pressure on the internal forces of the metro station should be first serious considered until the burial depth of the metro station increasing to a specific extent.

From the above we can see that when the burial depth of the metro station increases gradually, the bending moment and shearing force at critical nodes are in an increasing trend. When the burial depth of the station increases to a specific extent, the increasing trend of the bending moment and shearing force at critical nodes will slow down, and the displacement and dynamic amplification factor of roof and side wall show a negative growth.

4 SAKING TABLE TEST OF METRO STATION

From the above section, we may know near-field seismic action has the most influence on the dynamic response of the metro station. The internal forces of the metro station are the greatest when the burial depth is 25m. For this reason, we did a shaking table test of progressive failure of the metro station under near-field earthquake (T2-II-1) when the burial depth is 25m. We could determine the failure mode and failure position of the metro station by the test.

4.1 Design of test model

The dimension of the model is determined according to the dimension of the shaking table. The dimension of the shaking table is 1.5m×1.5m, the dimension of the model box is 0.5m (wide) ×2m (length) ×1.5m (height), and the test model is shown in Figure 8. The geometric similarity coefficient is set as 1:50, and other specific similarity coefficients are shown in Table 4. 20mm thick sponge was laid on the inner wall of the model box to reduce reflection of seismic waves on the boundary. Before the test, white noise was adopted for shock excitation on the top of the shaking table to tamp the soil.



Table 4 –The main similarity constants of the model

| Type | Physical quantity | Similarity relation | Metro station | Site soil |
|----------------------------|-----------------------------|----------------------------------|---------------|-----------|
| Geometrical characteristic | Length | S_L | 1/50 | 1/4 |
| | Linear displacement | $S_r = S_L$ | 1/50 | 1/4 |
| | Equivalent density | $S_\rho = S_E / (S_L \cdot S_a)$ | 25/2 | 1 |
| | Elasticity modulus | S_E | 1/4 | / |
| Material Characteristic | Shear wave velocity | S_v | / | 1/2 |
| | Shear modulus of soil | S_G | / | 1/4 |
| | Overburden pressure of soil | $S_{\sigma'} = S_L S_g S_\rho$ | / | 1/4 |
| | Frequency | $S_w = 1 / S_t$ | 7.14 | 2 |
| | Acceleration | S_a | 1 | 1 |
| Dynamic characteristic | Time | $S_t = \sqrt{S_L / S_a}$ | 0.14 | 1/2 |
| | Dynamic stress | $S_\sigma = S_L S_a S_\rho$ | 1/4 | 1/4 |

a) Shaking table



b) Test model

Figure 8 –Shaking table test model of metro station

Owing to the complexity and particularity of soil, it is difficult to make soil and structure conform to the consistent similarity relations in model test. During the design of the test, only some non-critical similarity ratios were allowed to have distortion to assure the studied key issues conform to the similarity relations. The research of the shaking table test focused on dynamic response and failure mechanism of the metro station structure, so metro station structure's compliance with the requirement of similarity ratio was mainly considered. The following different basic physical variables were selected: length, elasticity modulus and acceleration for model structure, shear wave velocity, density and acceleration for model soil, as shown in Table 4.

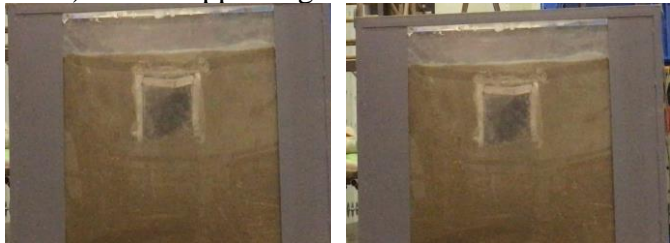
| | | | | |
|--|----------------|--|---|---|
| | Dynamic strain | $S_\varepsilon = S_L S_a S_\rho / S_E$ | 1 | 1 |
|--|----------------|--|---|---|

4.2 Failure Mode of the metro station structure

The peak acceleration of the earthquake is increased continuously on a margin of 0.1m/s^2 till failure of the metro station structure. During vibration, the progressive damage and failure of the metro station are video recorded. Due to restricted conditions, only the pictures of station failure are shown in Figure 9.



a) Cracks appearing of the metro station roof



b) Vertical deformation and collapse of the metro station roof



c) Collapsing destruction of the metro station roof

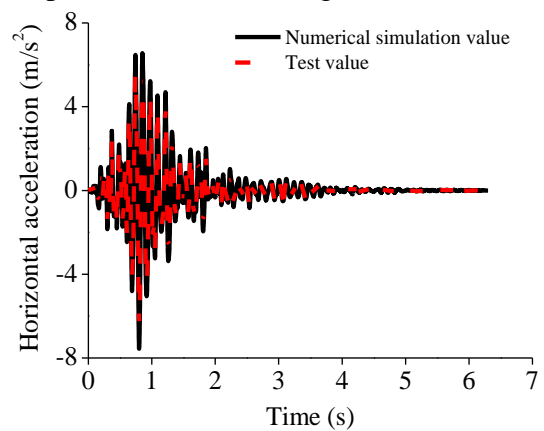
Figure 9 –Progressive failure mode of metro station

As shown in Figure 9, cracks first appeared at the junctions between the roof and side walls under earthquake T2-II-1. With the continuous action of the earthquake, cracks appeared on the middle of the roof and gradually the roof began to sink. At last, the cracks spread, eventually the roof collapsed and the metro station was fully destroyed under the joint effect of the seismic action and the gravity of the roof. Thus, after shear failure, the inertial effect of overlying soil significantly increases the vertical load on the roof. Under the combined influence of earthquake and overlying soil, the metro station eventually collapsed and failed. The main reason is that seismic waves spread at the bottom and the seismic amplification effect took place when they pass through the soil layer to enhance the seismic effect of the roof position. Particularly, vertical tensile de-

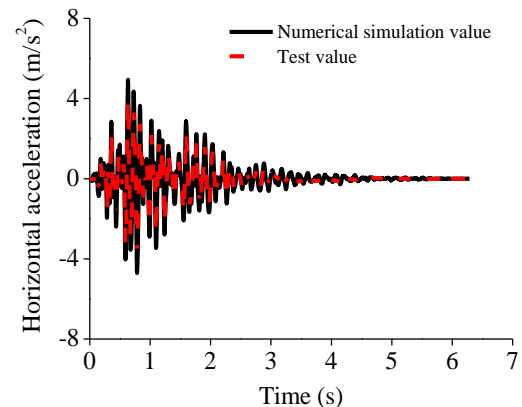
formation of the roof generated under earthquake under the combined action of earthquake and overlying soil pressure of the roof. Besides, the junctions between roof and side walls were vulnerable positions, so tensile failure happened at first, causing overall failure of the metro station at last.

4.3 Results comparison of numerical simulation and indoor test

The acceleration time histories of the middle monitoring point 7 on the roof and monitoring point 6 on the side wall with burial depth 25m were selected and compared, as shown in Figure 10.



a) Acceleration time history of the monitoring points 7 on the roof (burial depth 25m)



b) Acceleration time history of the monitoring point 6 on the side wall (burial depth 25m)

Figure 10 –Comparison between numerical simulation results and test results

As shown in Figure 10, the horizontal acceleration of the roof mid node obtained from numerical simulation and the horizontal acceleration time history obtained from the monitoring in a shaking table test were compared and analyzed, and the calculation results of the numerical simulation are greater than the horizontal acceleration measured in the shaking table test as a whole. However, the numerical simulation results are in good agreement with the experi-

mental results. The errors are all controlled within 20%. Thus, the accuracy of numerical simulation results is verified. The numerical simulation results are relatively great mainly because the acceleration conductors adopted in indoor test have signal attenuation, which would generate certain error to the test results.

5 CONCLUDING REMARKS

1. The displacement and acceleration amplification factor of the metro station show a decreasing trend when the burial depth increases gradually. The influence of burial depth on displacement and acceleration amplification factor of the metro station decreases when the burial depth reaches a specific value (the depth in this article is 20m). And the influence of burial depth on the displacement and acceleration amplification factor of the metro station could be omitted after a specific value of the burial depth. Near field earthquake has greater influence on the displacement and dynamic amplification factor of the metro station than far field earthquake.
2. The burial depth has great influence on the internal force of the metro station structure within a certain depth range. With the increase of burial depth, the influence of earthquakes on the internal forces of the metro station structure decreases while the influence of overlying site pressure on the internal forces increase gradually. Therefore, the influence of the overlying site pressure on the internal forces of the metro station should be first serious considered after the burial depth of the metro station increasing to a specific extent.
3. The failure mode of metro station is investigated by shaking table test, and we found that cracks first appeared at the junctions between the roof and side walls under earthquake. With the continuous action of the earthquake, cracks appeared on the middle of the roof and gradually the roof began to sink. Then the cracks spread and eventually the roof collapsed and the metro station was fully destroyed under the joint effect of the seismic action and the roof gravity. At last, shaking table test results demonstrate the validation of the numerical simulation results.

ACKNOWLEDGMENTS

This work is financially supported by the National Natural Science Foundation of China (Grant No. 51708516), National Key R&D Program of China (2017YFC1500404), Beijing Natural Science Foundation (Grant No. 8174078), and research grant from Institute of Crustal Dynamics, China Earthquake Administration (No. ZDJ2017-28)

REFERENCES

1. Quan D Z., Wang Y H., Jing Y L., Zhou S H. and Zhang Y C. Review of anti-seismic structures of subway in loess area. *Technology for Earthquake Disaster Prevention*, vol. 10, issue 3, 2015, pp, 565-574.
2. Du X L., Wang G., Du D C. Earthquake damage mechanism analysis of DaKai Metro Station by kobe Earthquake. *Journal of Disaster Prevention and Mitigation*, vol. 36, issue 2, 2016, pp, 166-171.
3. Ou Y Y Q., Ma S C. Dynamic Response Analysis of Underground Structures Subjected to Earthquakes Occurring Directly Beneath the Structure. *Soil Engineering and Foundation*, vol. 23, issue 6, 2009, pp, 68-70.
4. Li X Y. The Response Characteristic Research of Shallow-tunnel Timbering Structures under Earthquake Loads. Xi'an University of Science and Technology, 2011.
5. Hashash Y., Hook J J., Schmidt B. Seismic design and analysis of underground structure. *Tunnelling and Underground Space Technology*, vol. 16, issue 4, 2001, pp, 247-293.
6. Gazetas G., Gerolymos N., Anastopoulos I. Response of three Athens metro underground structures in the 1999 Parthenon earthquake. *Soil Dynamics and Earthquake Engineering*, vol. 25, issue 7, 2005, pp, 617-633.
7. Youssef M A., Jeffrey J., Birger S, John I-Chiang Y. Seismic design and analysis of underground structures. *Tunnelling and Underground Space Technology*, vol. 25, issue 7, 2005, pp, 247-293.
8. LIU J B, LI B. Issues on the seismic analysis and design of subway structures. *China Civil Engineering Journal*, vol. 39, issue 6, 2006, pp, 106-110.
9. LIU J B, LIU X Q, DU X L. Prospects for the development in theoretical analysis and experimental study of seismic response of underground structures. *Journal of Earthquake Engineering and Engineering Vibration*, vol. 27, issue 6, 2007, pp, 38-45.
10. Deng C J, He G J, Zheng Y G. Studies on Drucker Prager yield criteria based on M-C yield criterion and application in geotechnical engineering. *Chinese Journal of Geotechnical Engineering*, vol. 28, issue 6, 2006, pp,735-739.
11. Specifications for highway bridges part V: seismic design 1st Ed[S]. Japan: Japan Road Association, 2002.